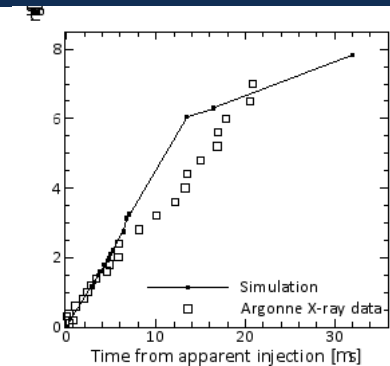
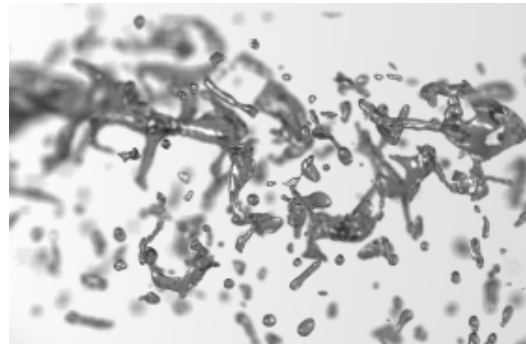
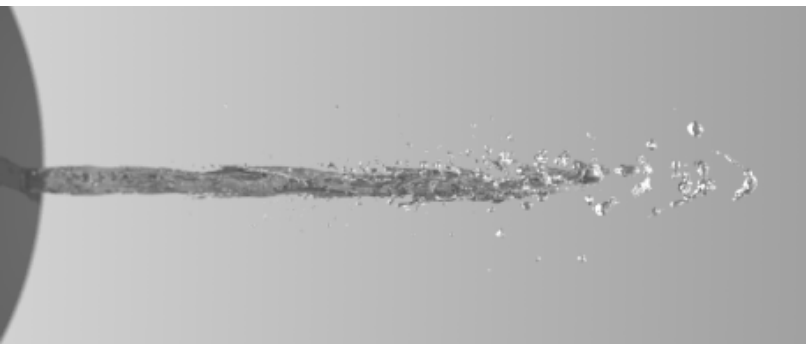


Exceptional service in the national interest



Compressibility effects in the initial transient of high-pressure Diesel injection

Marco Arienti^a and Mark Sussman^b

(a) Sandia National Laboratories
(b) Florida State University

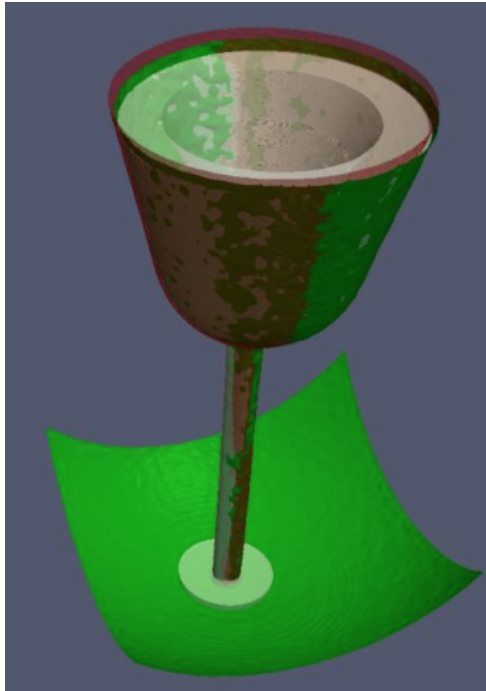


Sandia National Laboratories is a multi-program laboratory managed and operated by Sandia Corporation, a wholly owned subsidiary of Lockheed Martin Corporation, for the U.S. Department of Energy's National Nuclear Security Administration under contract DE-AC04-94AL85000. SAND NO. 2011-XXXXP

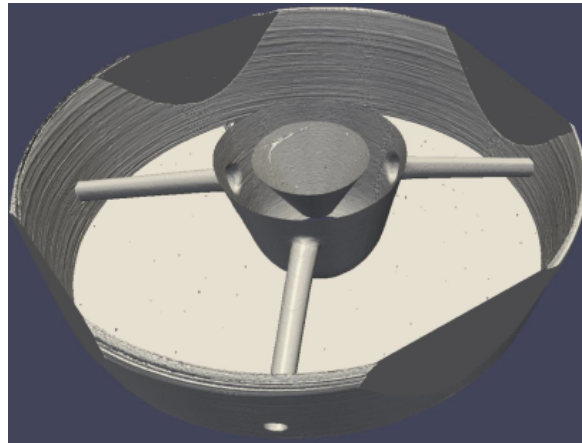
A family of fuel injectors

Go to the *Engine Combustion Network* webpage:

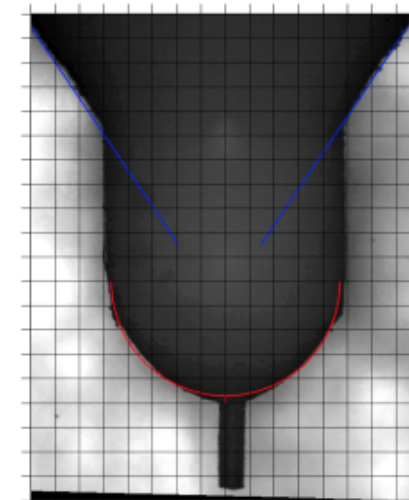
<http://www.sandia.gov/ecn/index.php>



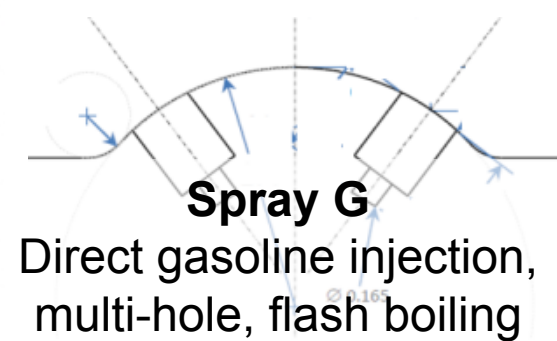
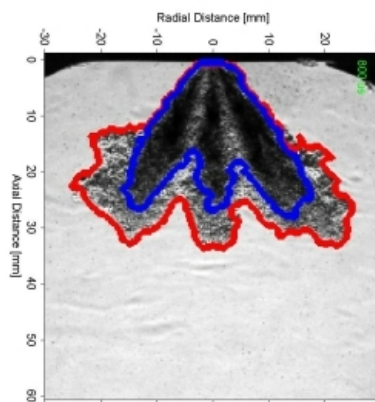
Spray A
Diesel (n-dodecane),
single hole,
mildly or not cavitating



Spray B
Diesel, multi-hole



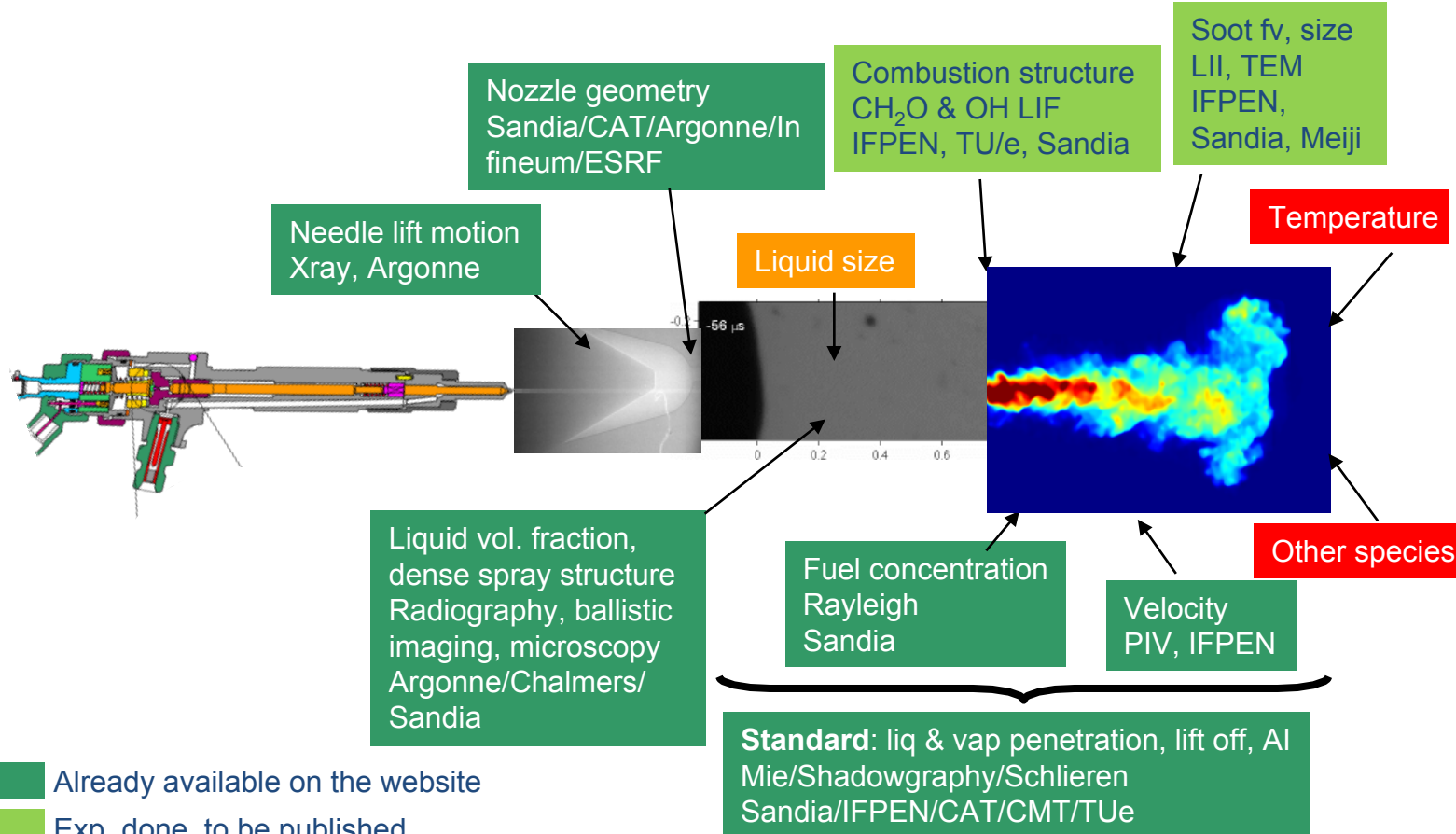
Spray H
Diesel (n-heptane), single hole,
prone to cavitation



Spray G
Direct gasoline injection,
multi-hole, flash boiling

Spray A effort: a snapshot (April 2014)

*30+ different measurements by 10+ different institutions
15 years of research performed in 3 years*



Already available on the website

Exp. done, to be published

In progress

Considered

Computational features

Starting point: the Combined Level Set Volume of Fluid (CLSVOF) method

- “A sharp interface method for incompressible two-phase flows”
Sussman et al. J. Comp. Phys. (2007)

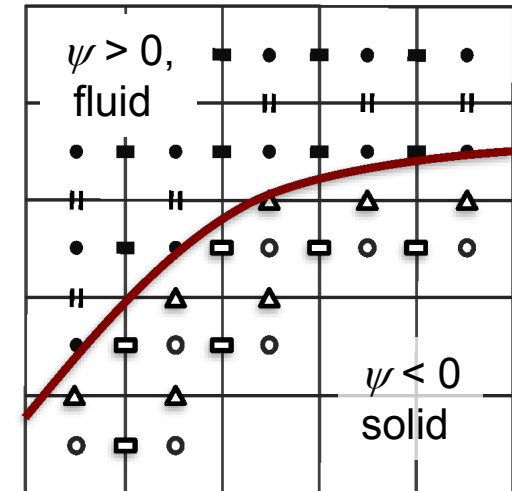
Additional / revamped features:

- An embedded boundary approach for complex geometries
- Directionally split Eulerian-Implicit Lagrangian-Explicit (EI-LE) advection
- Compressible formulation of Poisson solver step
- The Moment-of-Fluid (MOF) formulation

The embedded solid boundary

A simple level set-based staircase approach

- The solid boundary is represented as the zero level set of a signed distance function, ψ .
A “solid face” has $\psi_{i,j,k} \cdot \psi_{i+1,j,k} < 0$
- ψ is calculated from a given triangulation (mesh) of the body surface: when N solid bodies exist, $\psi = \min(\psi^1, \psi^2, \dots \psi^N)$
- In case of solid motion, ψ and wall node normals \mathbf{n}_{node} are recalculated at every iteration
- The components of flow velocity at the wall are made consistent with the no-slip boundary condition through the Poisson equation and the projection operator:
 $\mathbf{u}^* = \mathbf{v}$ so that $\nabla p \cdot \mathbf{n}_{face} = 0$ at solid faces
- The values of \mathbf{v} are extended into the ghost region by a front-advancing procedure where an unmarked cell takes its value from the neighboring cells that have already been marked

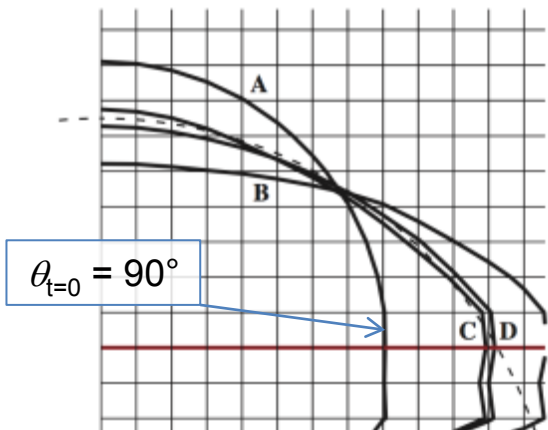


[Arienti and Sussman, IJNMF, 2014]

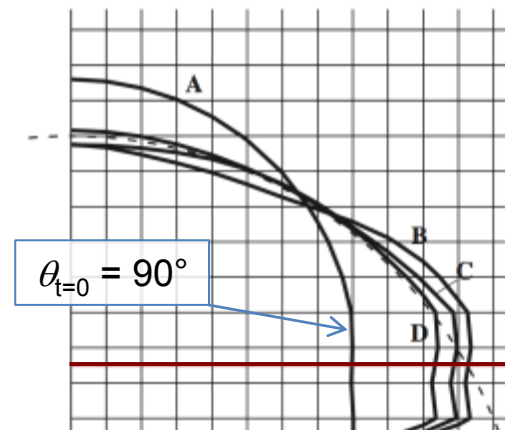
Contact point on solid surface

- The contact angle θ_w is prescribed
- The algorithm for curvature reverts to calculating the divergence of the interface normals near the contact point
- If the cell center falls in the solid region, \mathbf{n}_ϕ is replaced by $\mathbf{n}(\mathbf{n}_\psi, \theta_w)$

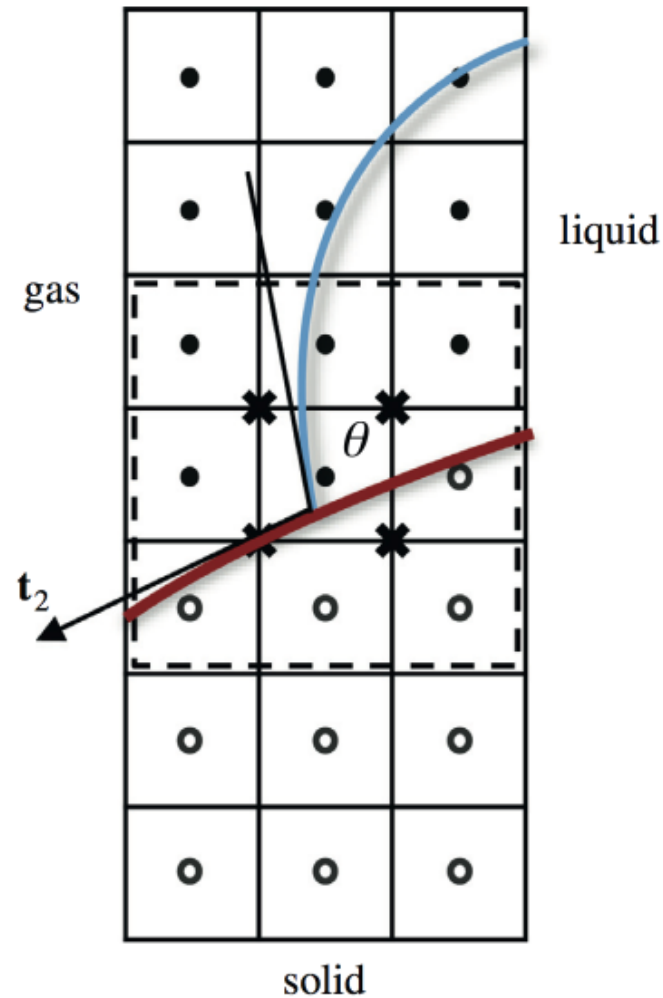
Effect of wall location for a drop with $\theta_w = 60^\circ$



Wall overlaps
the cell faces



Wall passes through
the cell centroids



Extension to compressible flow

Asymptotically preserves the incompressible pressure projection in the limit of infinite sound speed

- Evaluate the “advective pressure,” p^a and the “advective sound speed” $(c^2)_a$ (Kwatra, Su, Grétarsson, Fedkiw, J. Comput. Phys., 2009)
 - In a cut cell, p^a is evaluated from the equation of state for the material m^* that occupies **the largest volume fraction** in the cell

$$p_j^a = EOS^{m^*} \left(e_{int}^{m^*, a}, \rho^{m^*, n+1} \right)$$

- Solve for P^{n+1}

$$P^{n+1} - \rho^{n+1} \left(c^2 \right)^a \Delta t^2 \nabla \cdot \left(\frac{\nabla P^{n+1}}{\rho^{n+1}} \right) = p^a - \rho^{n+1} \left(c^2 \right)^a \Delta t \nabla \cdot \mathbf{u}^a$$

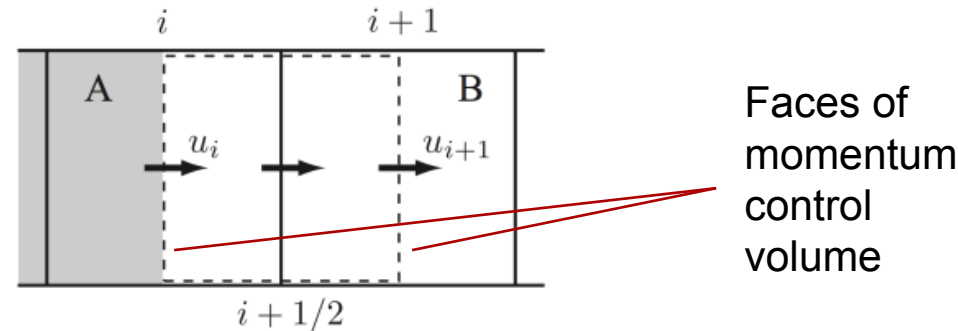
using mass-weighted interpolation of the cell centered \mathbf{u}^a

Consistency of mass and momentum advection (Sussman and Jamison)

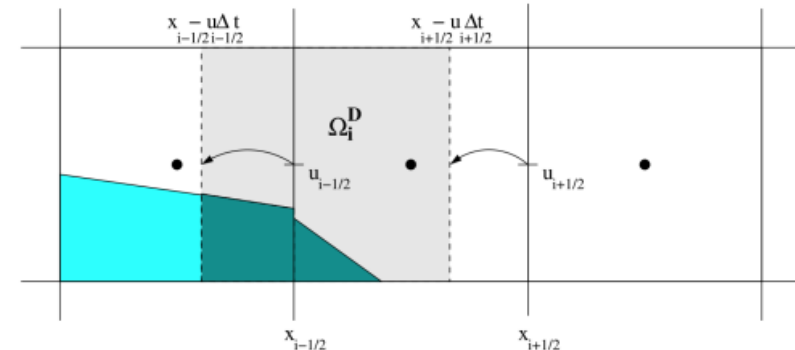
- The full Navier–Stokes equations for multimaterial flow are split in (1) advection and (2) semi-implicit pressure correction for momentum and energy
- The nonlinear terms in the momentum equations are solved using the momentum-conserving approach by Raessi and Pitsch (Annual Research Brief 2008)

Incoming momentum $\rho_A u_i \neq u_i \frac{\rho_A + \rho_B}{2}$

Face density $\rho_B \neq \frac{3}{4} \rho_B + \frac{\rho_A}{4}$



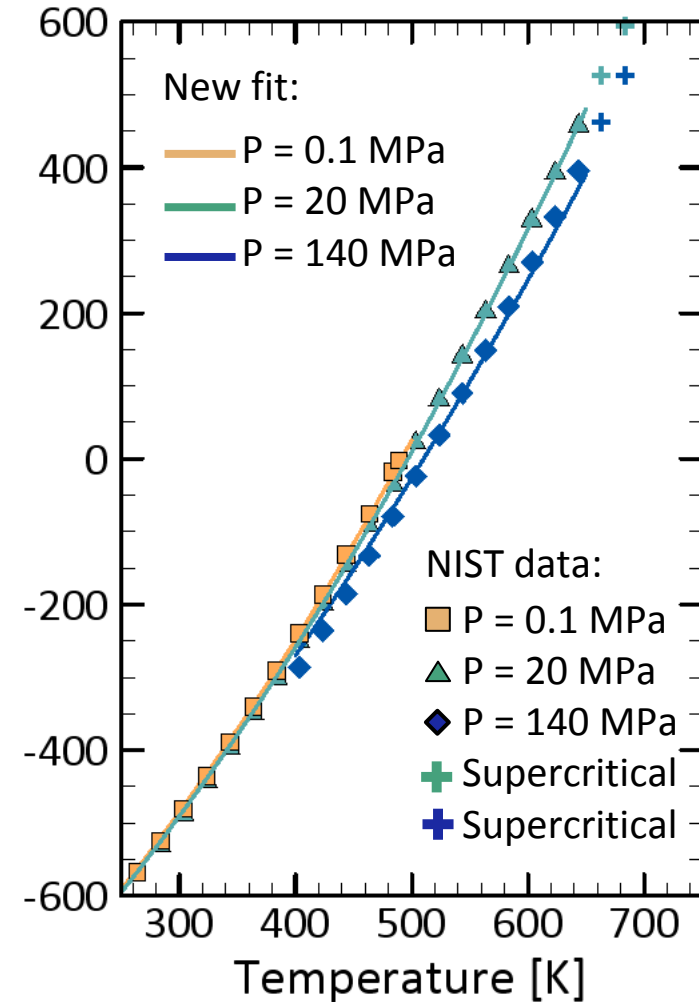
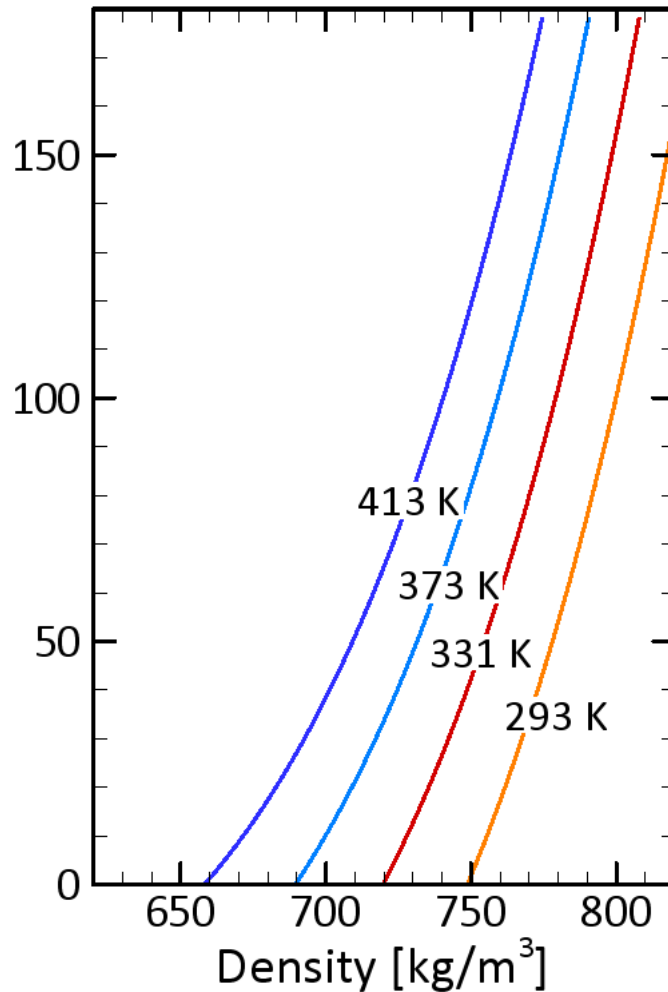
- Velocity is maintained and updated at both cell centers and face centers.
- In 1D use backward characteristic tracing



Equation of state of n-dodecane

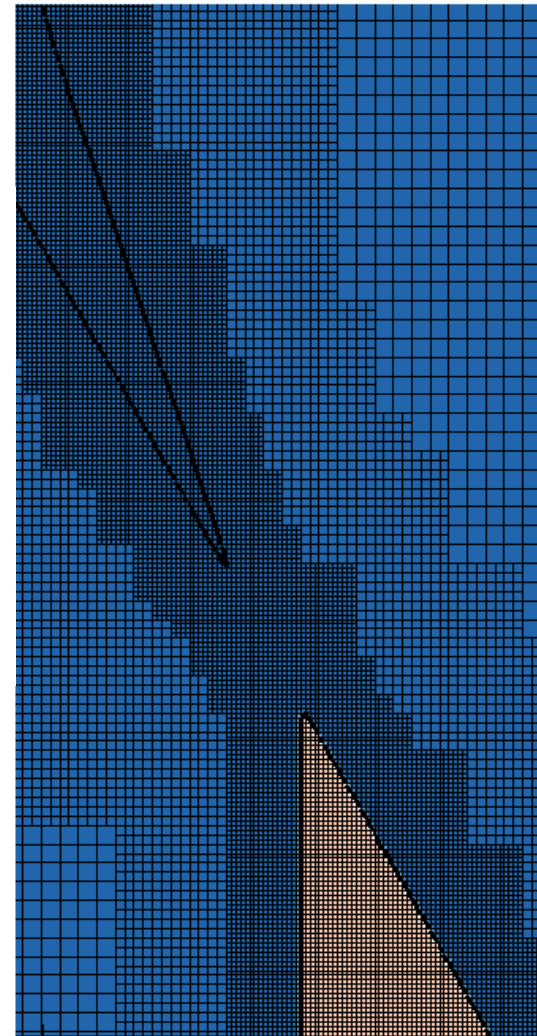
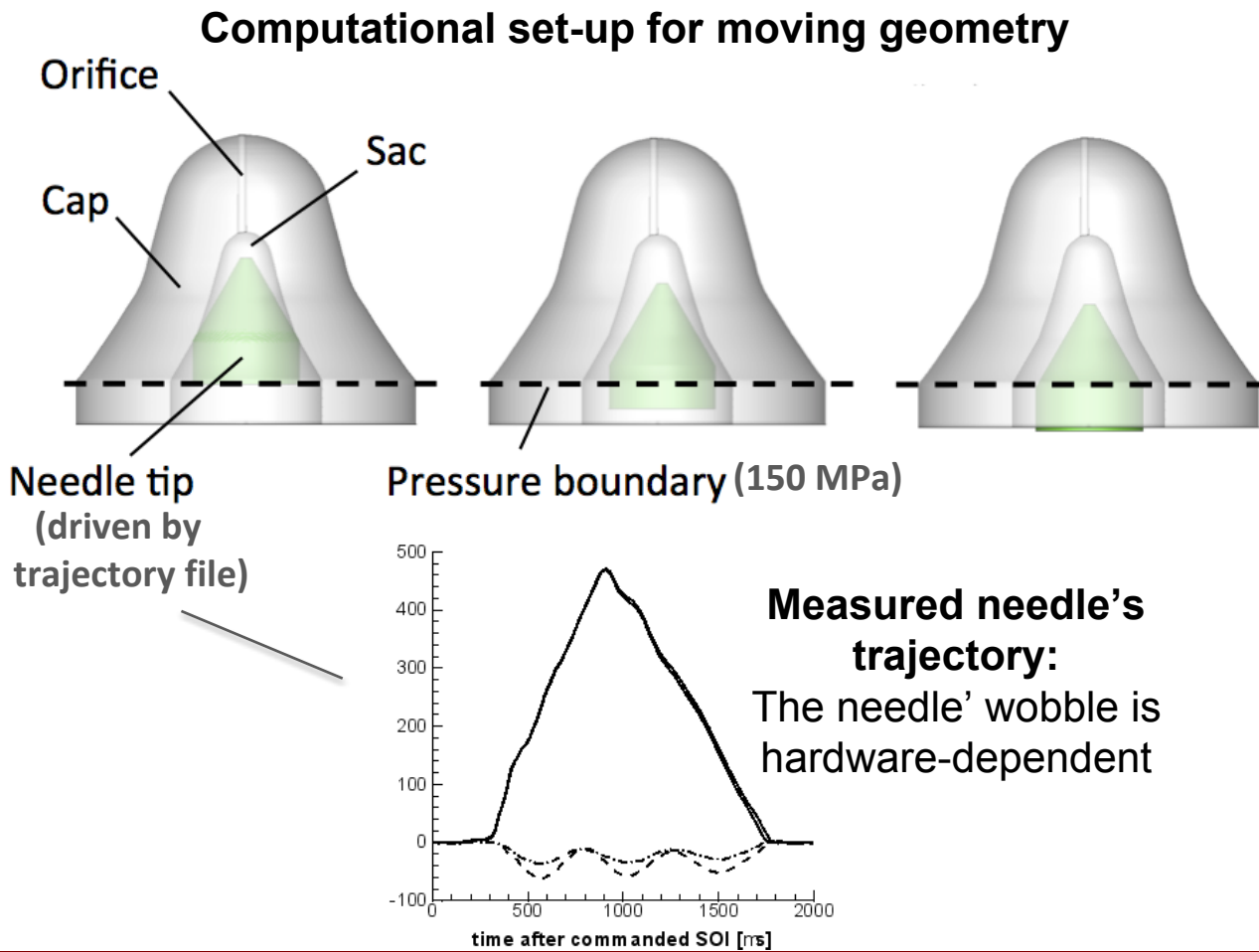
Calibrated Tait's EOS and a new $e(\rho, T)$ fit to data

■

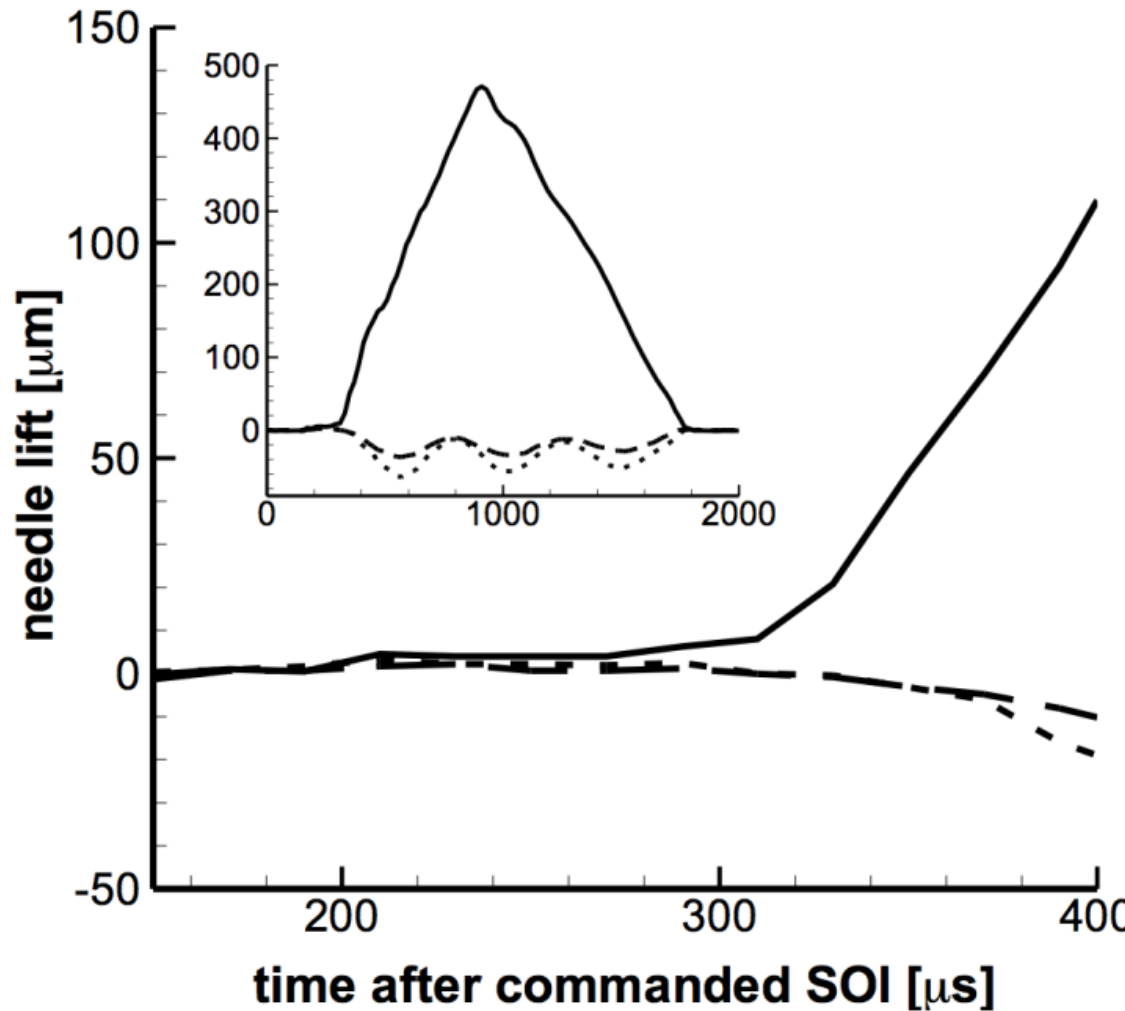


The needle's unseating

Successful pressure discharge following the needle's motion

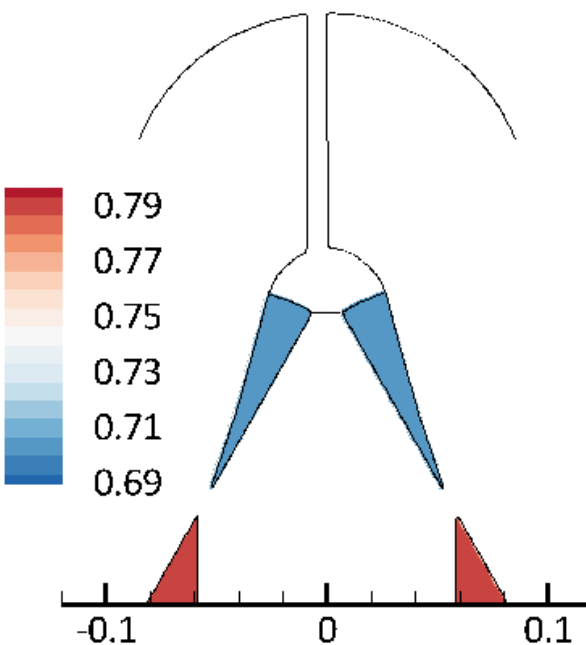


So far covered 339+35 μ s from
commanded start of injection (SOI)

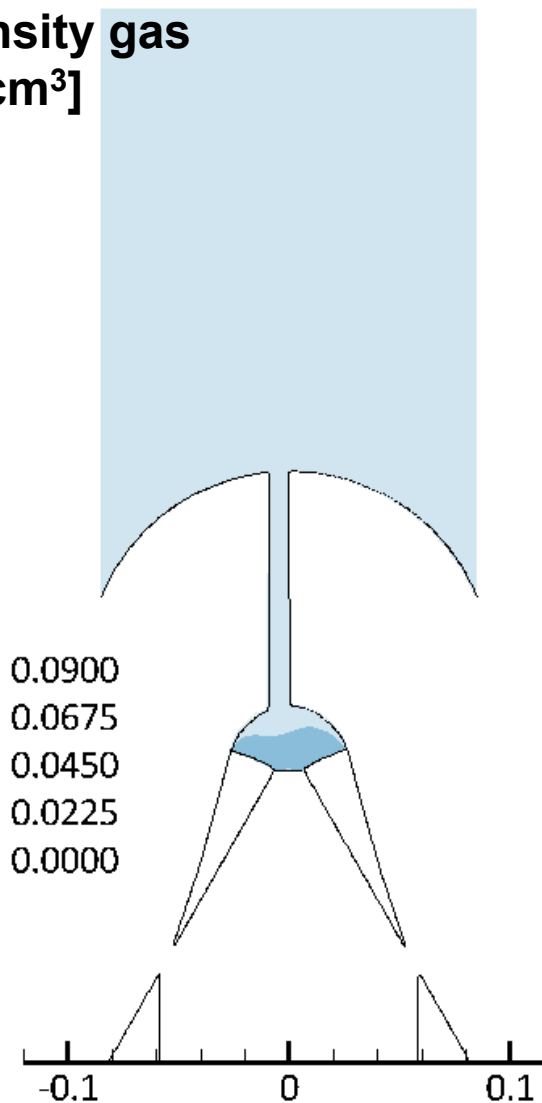


Dynamics of opening transient

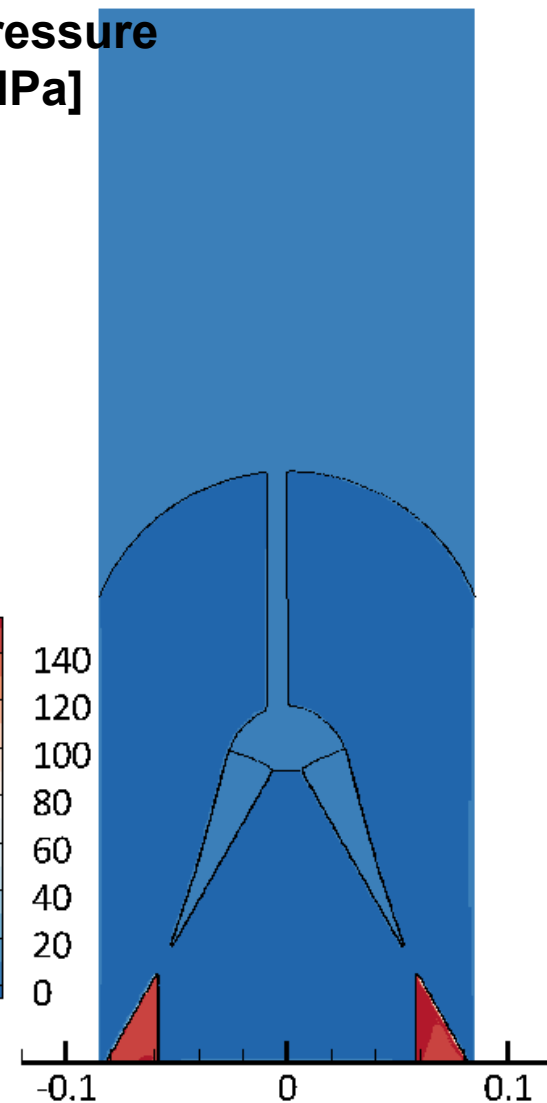
Density liquid
[g/cm³]



Density gas
[g/cm³]

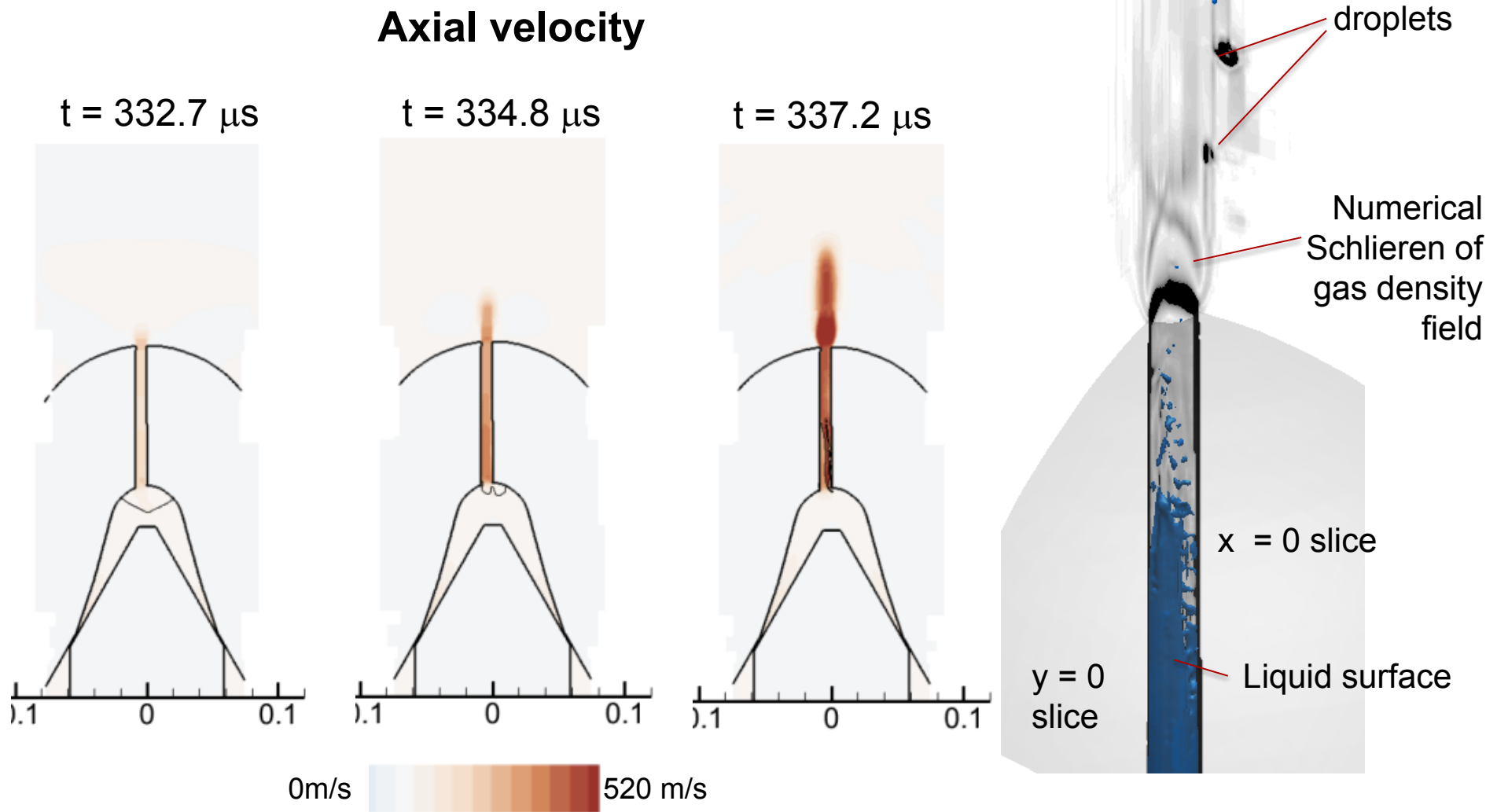


Pressure
[MPa]

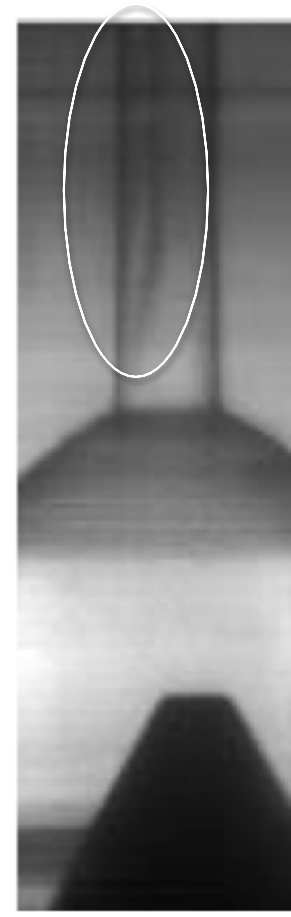
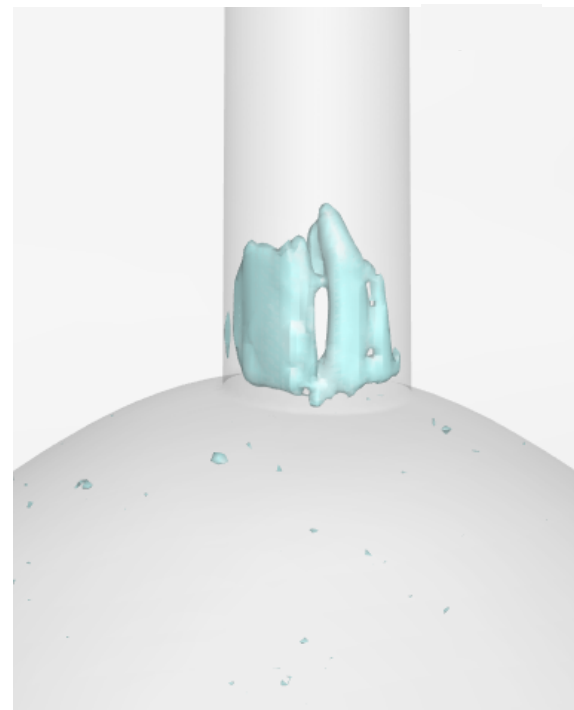


Under-expanded gas jet at the orifice

Example of multiphase supersonic flow



Evidence of trapped gas at the orifice

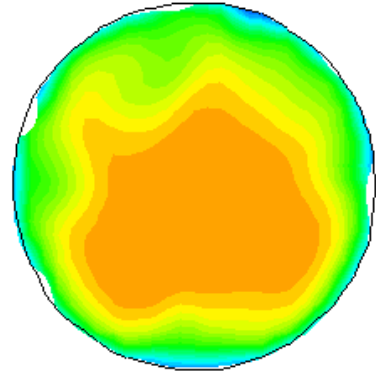


Transparent
injector (courtesy
of Ansgar Heilig,
Hannover)

- Estimated gas volume $\sim 3 \cdot 10^{-7} \text{ cm}^3 = 0.0015 V_{\text{vac}}$
- The average density of the gas inside the bubble is $\sim 0.2 \text{ g/cm}^3$
- The estimated residual gas mass is $\sim 6 \cdot 10^{-8} \text{ g}$

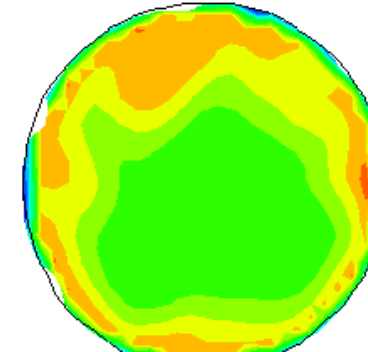
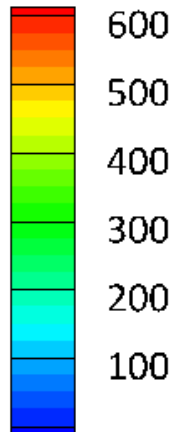
Flow cross-sections at the orifice

Turbulent and asymmetric flow, but over-estimated boundary layer



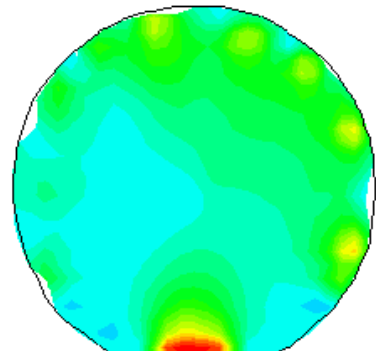
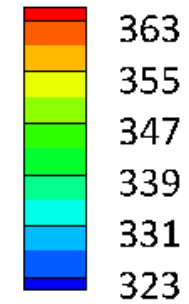
$t = 0.341195 \text{ ms}$

Axial velocity [m/s]



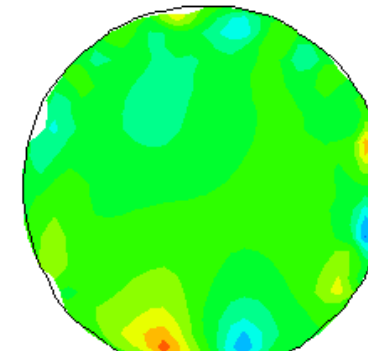
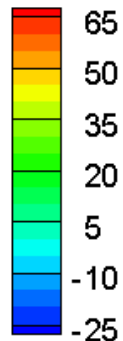
$t = 0.341195 \text{ ms}$

Temperature [K]



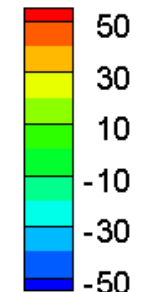
$t = 0.341195 \text{ ms}$

Radial velocity [m/s]



$t = 0.341195 \text{ ms}$

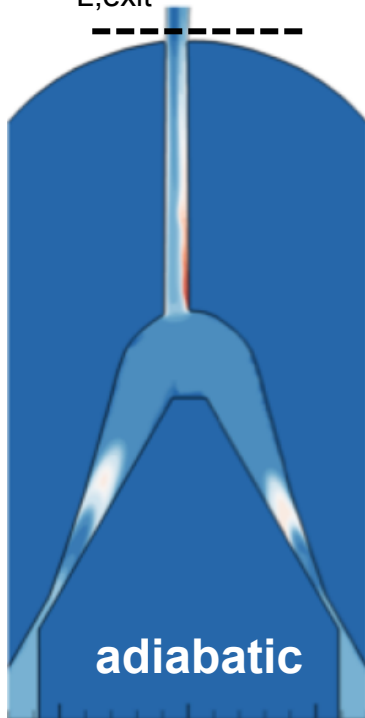
Tangential velocity [m/s]



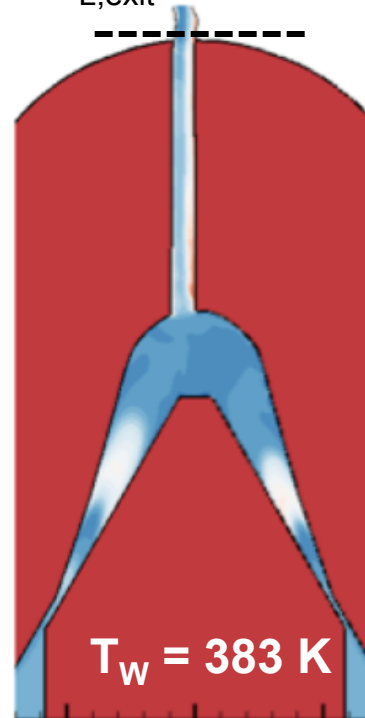
In progress: effect of wall heat transfer on fuel temperature

Observed limited temperature increase from $T_{L,0} = 343 \text{ K}$

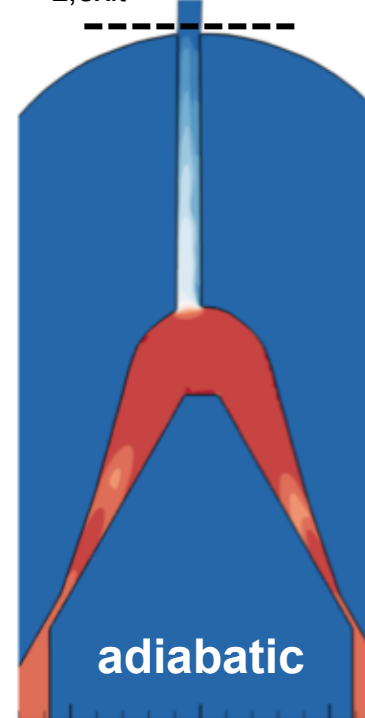
$$T_{L,\text{exit}} = 346 \text{ K}$$



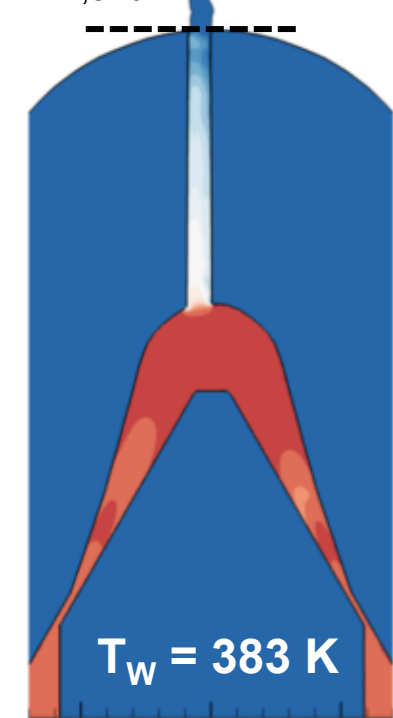
$$T_{L,\text{exit}} = 361 \text{ K}$$



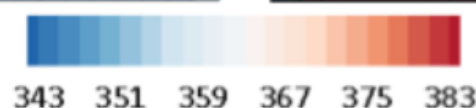
$$\rho_{L,\text{exit}} = 716 \text{ kg/m}^3$$



$$\rho_{L,\text{exit}} = 720 \text{ kg/m}^3$$



adiabatic



Liquid phase temperature [K]

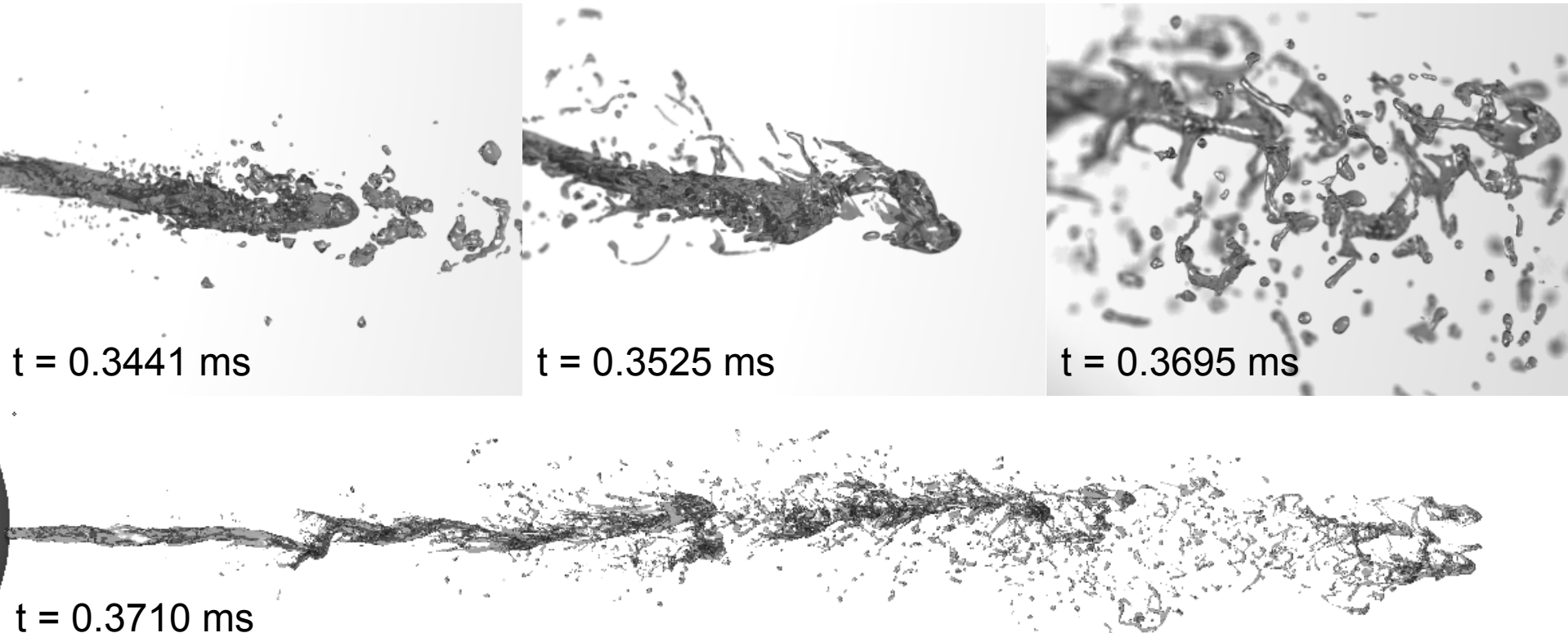
adiabatic



Liquid phase density [kg/m³]

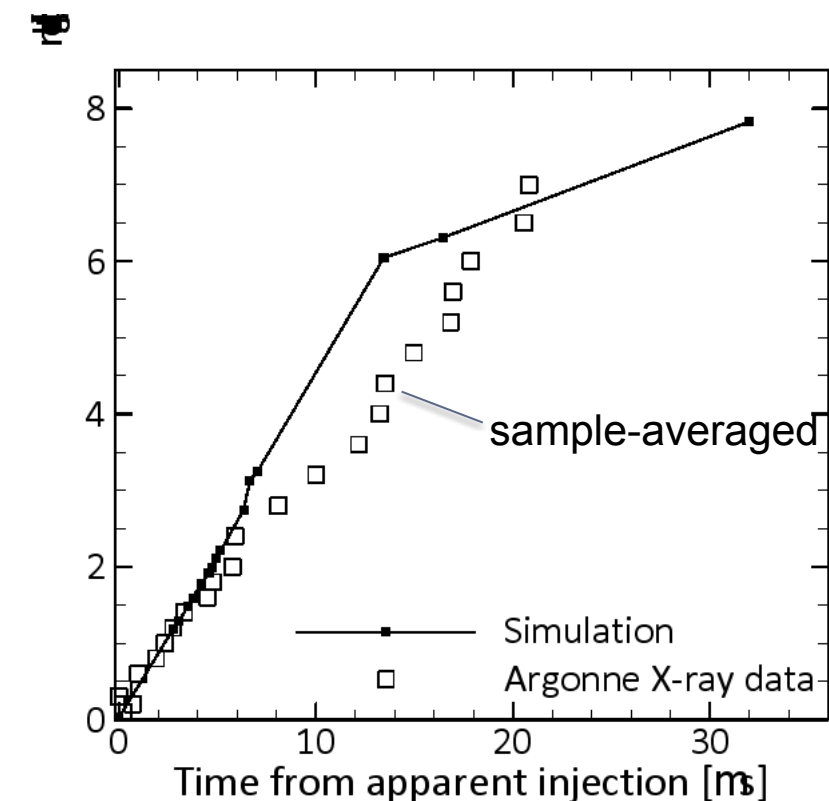
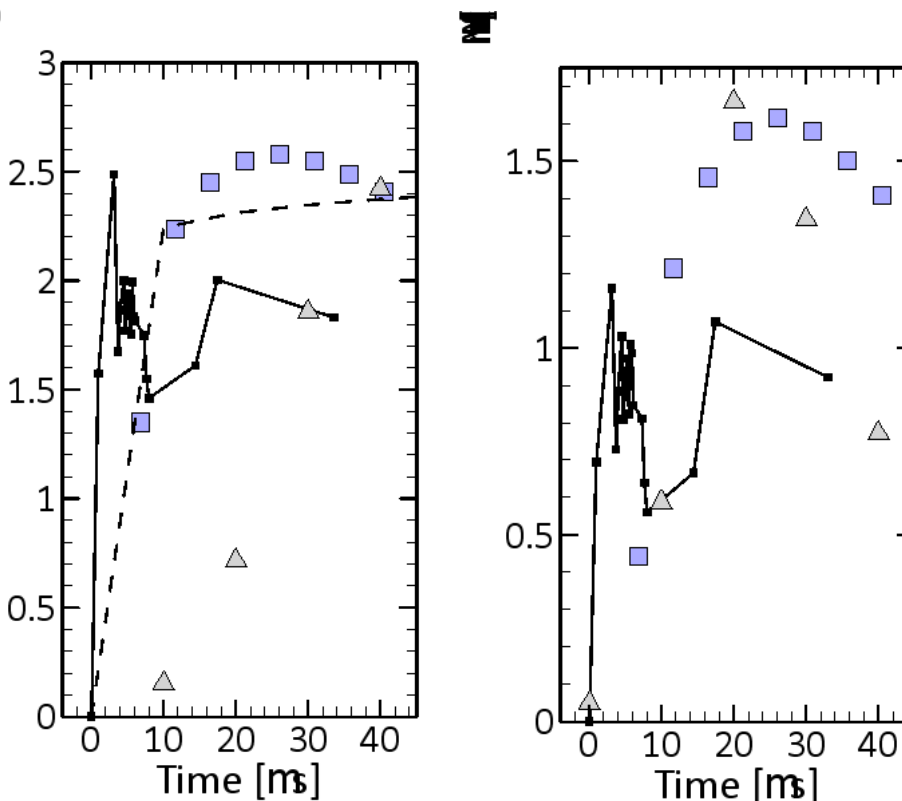
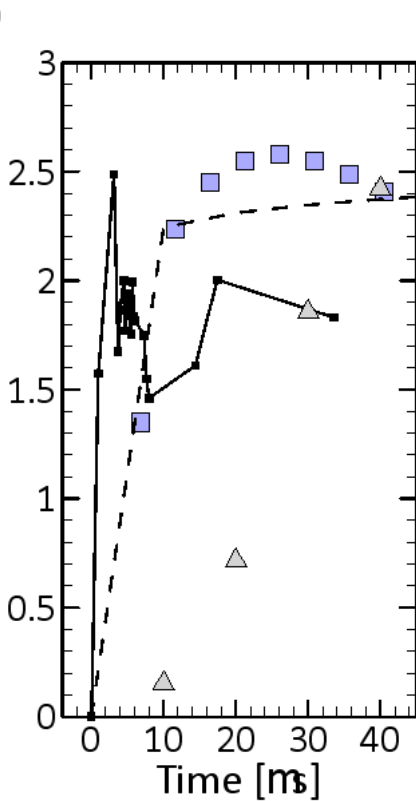
Jet tip structure

- Rapid disintegration of the jet
- No jet tip “mushroom” because of the internal flow dynamics



Flow rate and jet penetration

Transient flow rate and momentum flux below measured values, but reasonable agreement with penetration



- ▲ CMT measurements
- Sandia measurements
- - Model from filtered data
- This simulation

Nominal mass flow rate:
 $3.5\text{-}3.7\text{mg}/1.5\text{ ms} = 2.3\text{-}2.5\text{ g/s}$

Does simulation need to include manufacturing defects?

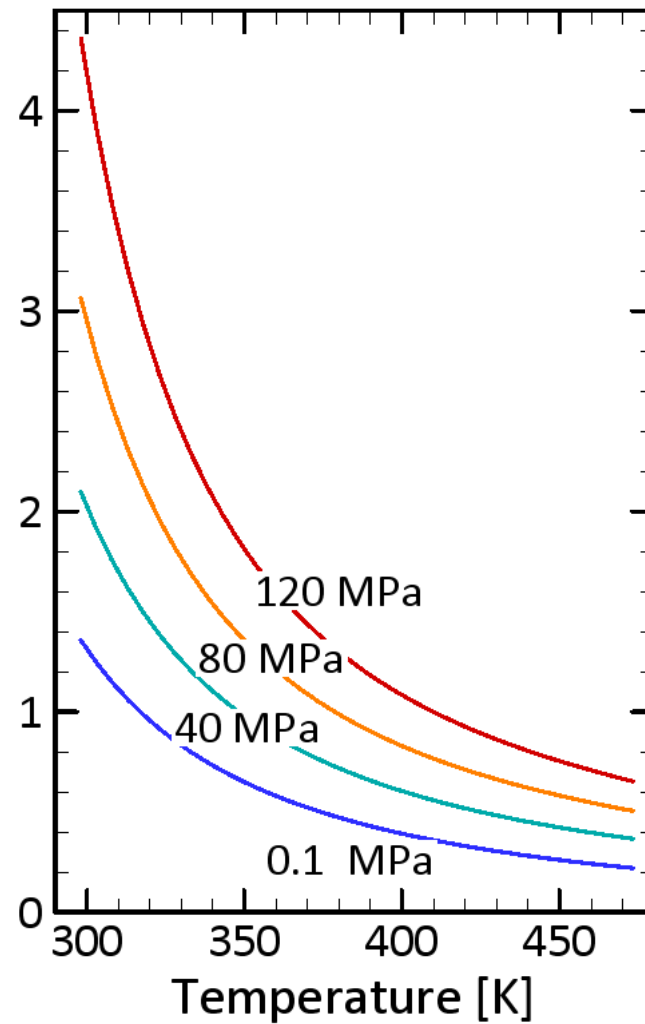
- Needle's wobble causes pressure distribution asymmetries at the orifice exit
 - Increasingly relevant with decreasing sac volume
- Perturbed liquid jet tip at the exit
 - Different from typical initial condition assumed for Diesel injection
 - No mushroom shape
- Misaligned orifice position causes asymmetric flow
 - Residual gas bubbles trapped at the orifice entry
- Partial fuel filling in the sac before unseating affects the time to apparent injection
 - One of the causes of cycle-to-cycle variability?

Questions?

Acknowledgements. The support by Sandia National Laboratories via the Laboratory Directed Research and Development program is gratefully acknowledged. Sandia National Laboratories is a multi-program laboratory managed and operated by Sandia Corporation, a wholly owned subsidiary of Lockheed Martin Corporation, for the U. S. Department of Energy's National Nuclear Security Administration under contract DE-AC04-94AL85000.

BACKUP

Dependence of viscosity on pressure

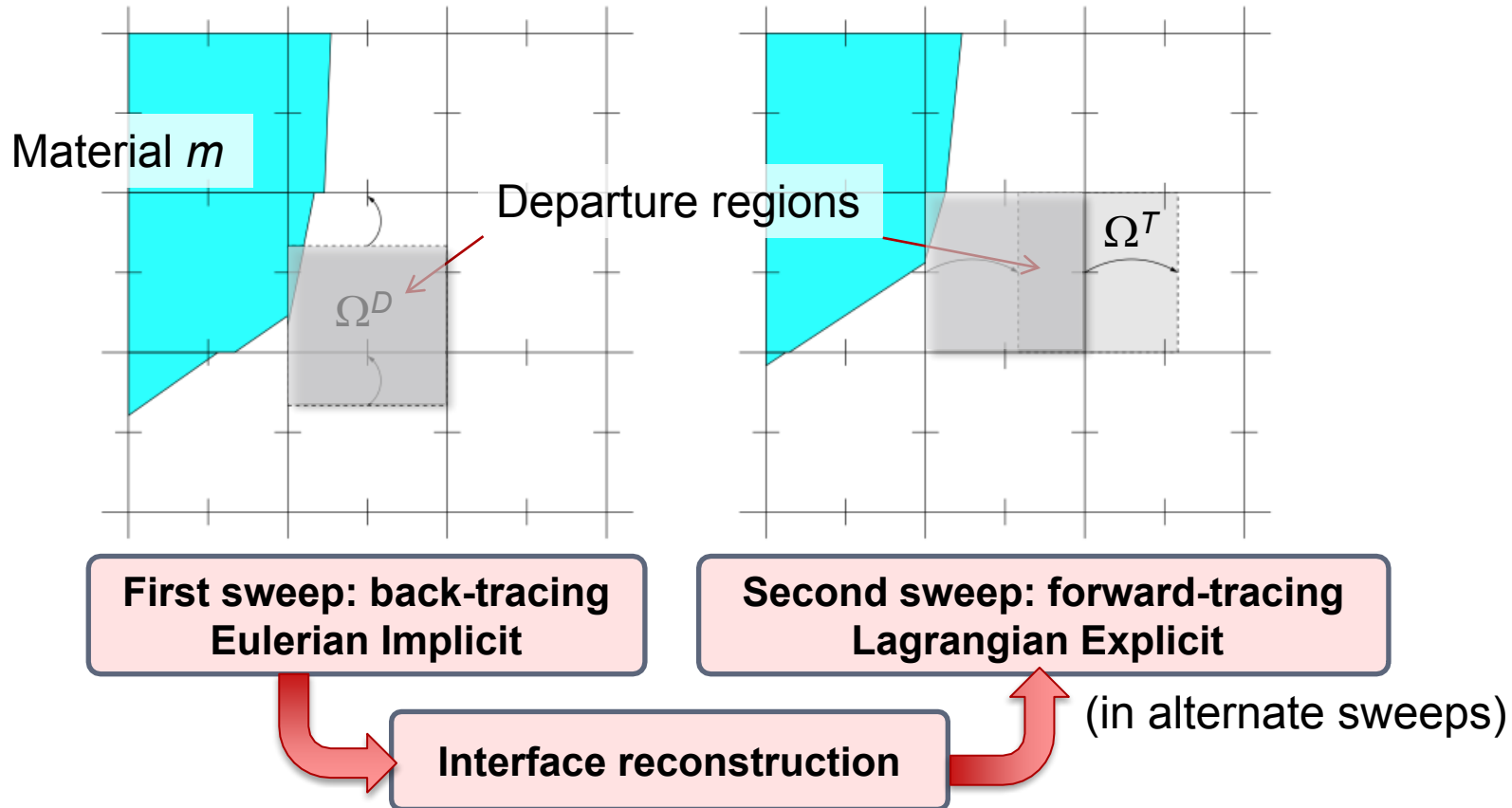


Conditions and setup

- “Argonne conditions” (cold flow): $T_L = 343$ K; $T_G = 303$ K
- Partially filled sac
- Back and ambient pressure: $P_L = 150$ MPa; $P_G = 2$ MPa
- Adiabatic walls, contact angle $\theta_w = 90^\circ$
- No turbulence models, no wall model
- Equation of state for n-dodecane compiled from data by Caudwell et al., Int. J. of Thermophysics, 2004; Khasanshin, et al., Int. J. of Thermophysics, 2003. Padilla-Victoria et al., Fluid Phase Equilibria 2013.
- Perfect gas EOS
- 64x64x576 coarse grid with 3 levels of refinement:
the finest grid resolution is $\Delta x_f = 3.32$ μm (~ 30 grid points across orifice)
adaptive stable time step $\Delta t \sim 2$ ns
- From 70 M to 210 M cells
- Run on Sandia’s redsky (from 64 to 168 dual socket/quad core nodes)

2D/3D: directionally split advection

Eulerian-Implicit/Lagrangian-Explicit (EI-LE)



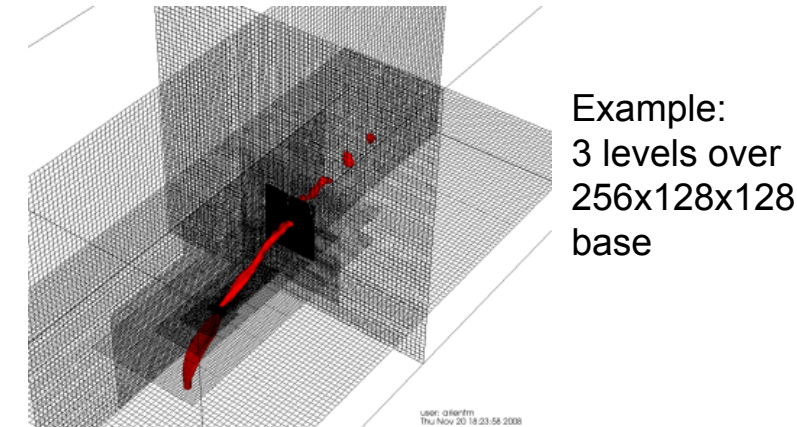
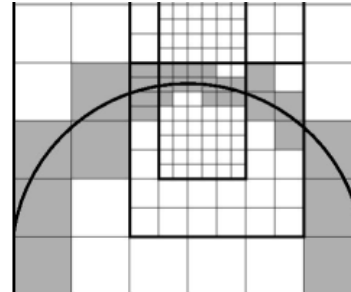
$$\Omega_{i,j}^D = [y_{j-1/2} - \Delta t v_{j-1/2}, y_{j+1/2} - \Delta t v_{j+1/2}] \quad \Omega_{i,j}^T = [x_{i-1/2} + \Delta t u_{i-1/2}, x_{i+1/2} + \Delta t u_{i+1/2}]$$

[Jemison, Sussman and Arienti, J. Comp. Physics 2013]

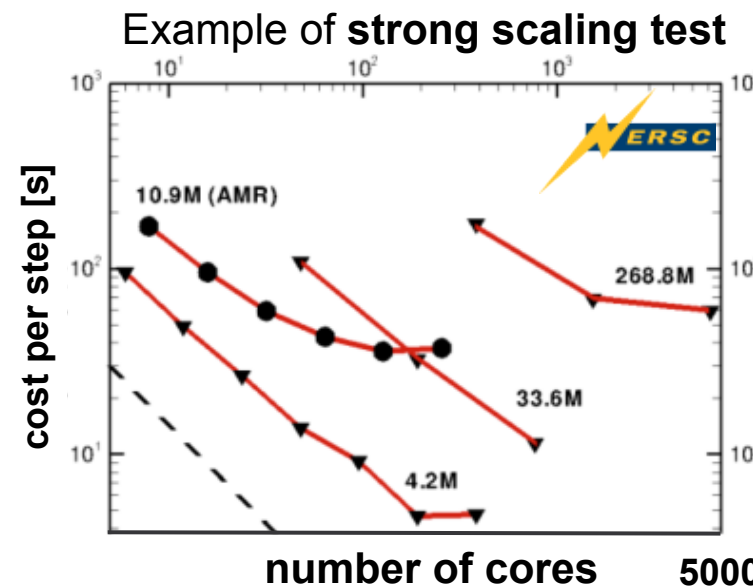
A box-structured data hierarchy

Adaptive mesh refinement and parallel structure managed by Boxlib
<https://ccse.lbl.gov/BoxLib/>

Proper nesting
(no more than one
level change at a
coarse/fine border)

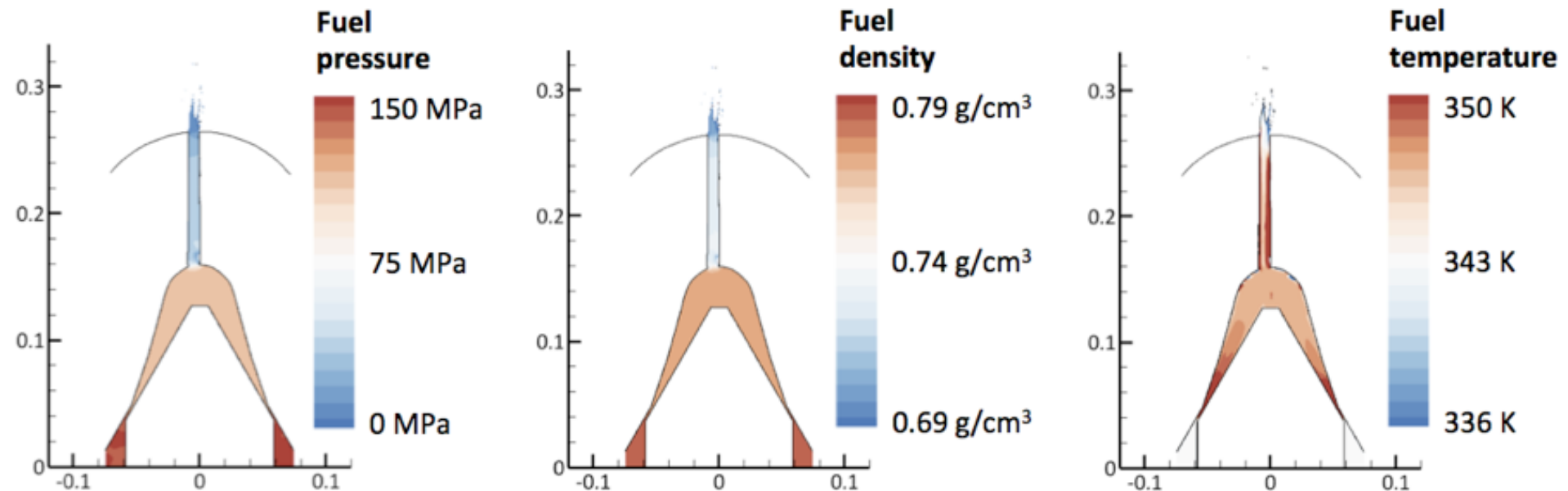


- AMR enables compact and efficient distribution of resources
- Data distribution and communication overhead limit scalability

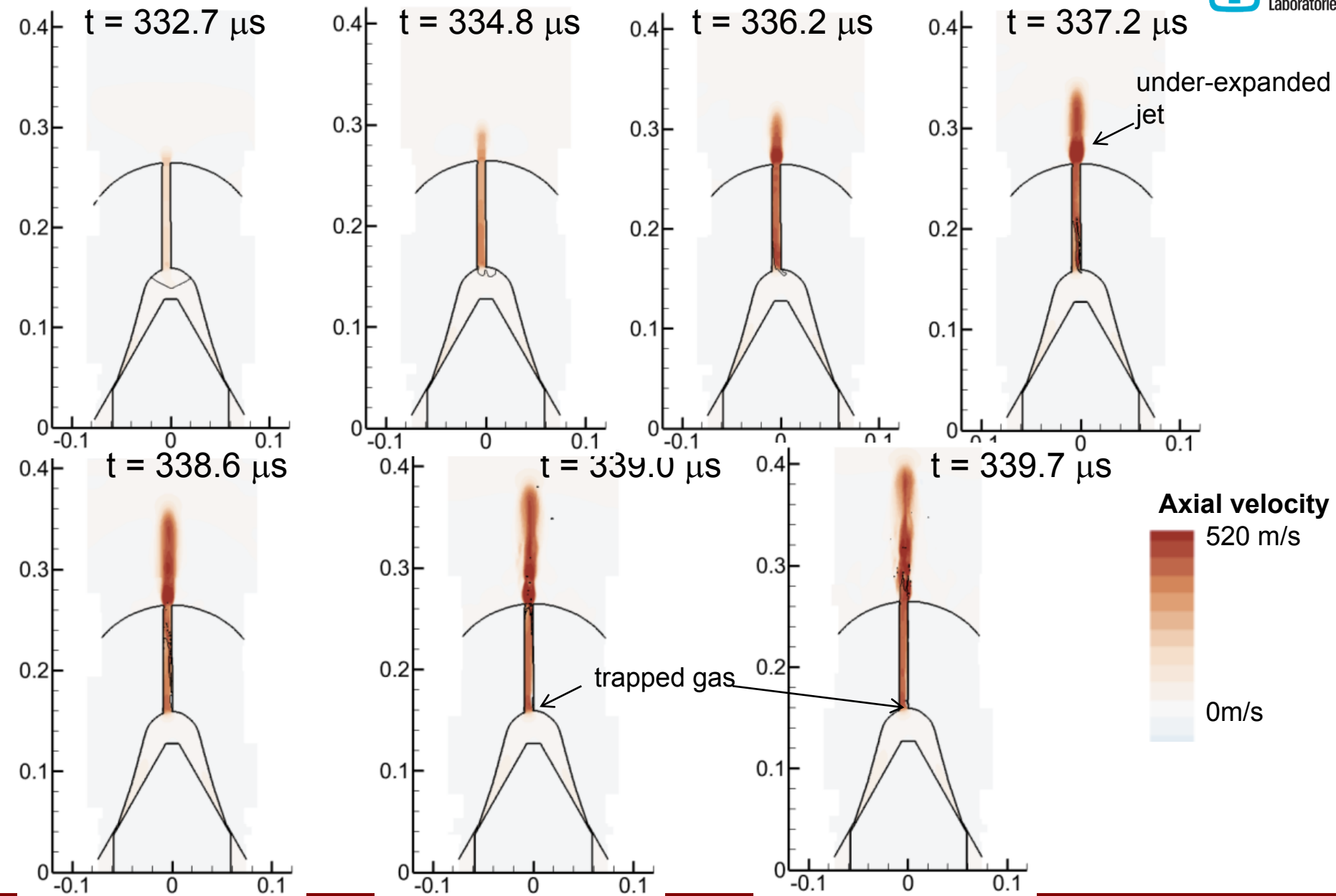


[Li and
Soteriou,
SciDAC
2011]

Pressure, density and temperature distribution of liquid fuel

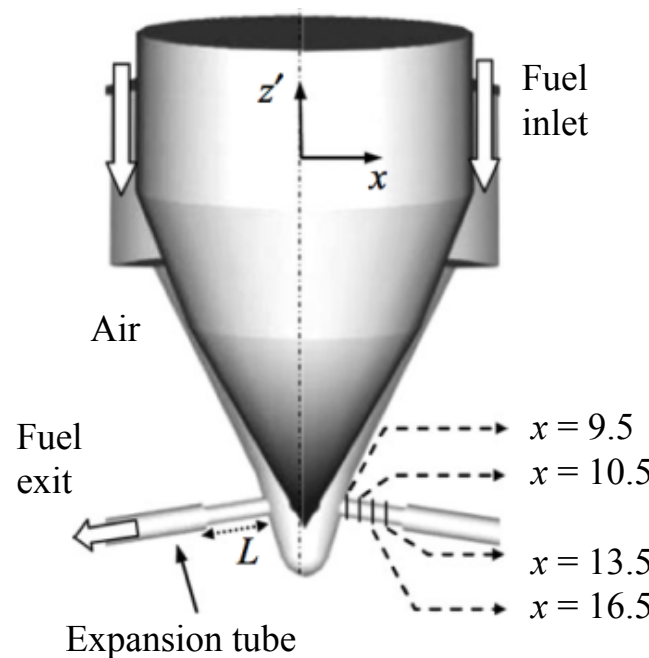


- Start of injection (SOI) from half-filled sac: $t = 0.339$ ms
- Adiabatic expansion of the liquid near the exit

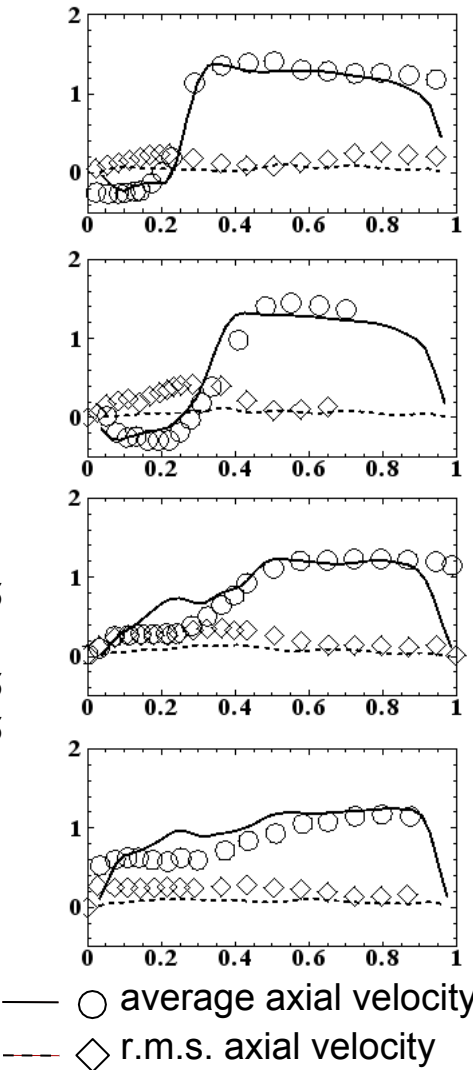


Validation: six-hole 20x Bosch Diesel injector

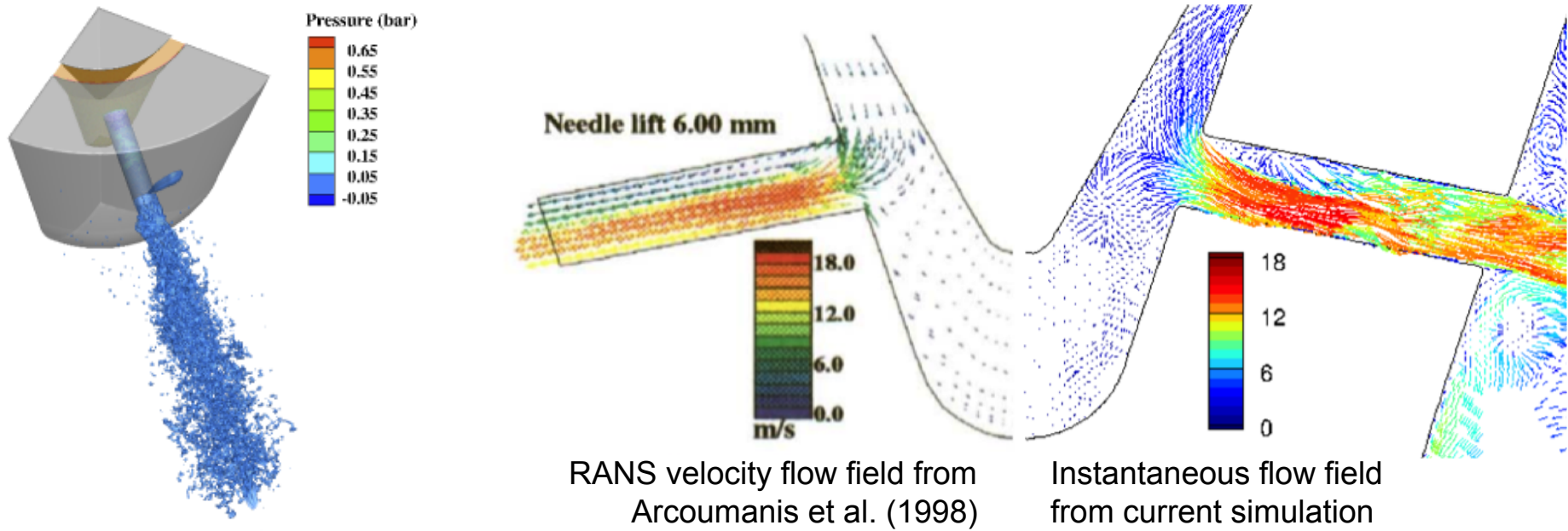
Positive match within the limits of under-resolved turbulence



[Arcoumanis et al., SAE Technical Series, 980911, 1998]

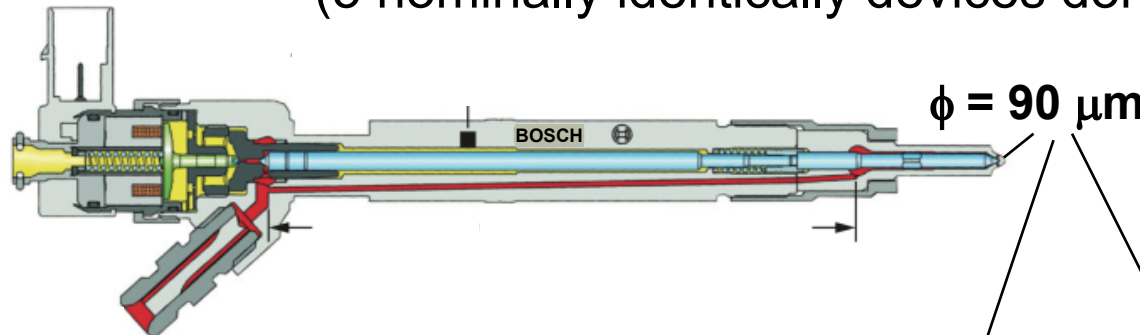


Six-hole 20x Bosch Diesel injector

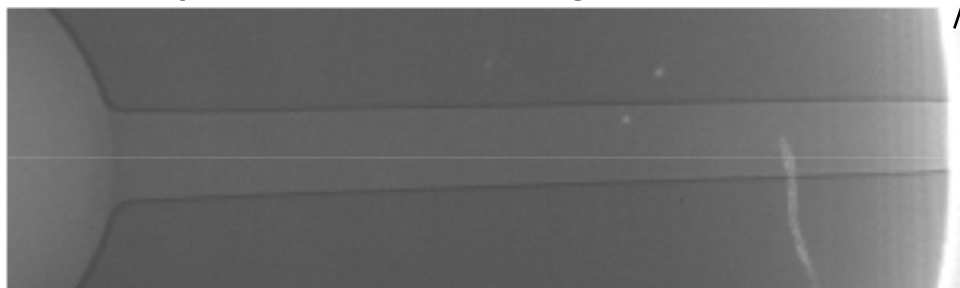


Does simulation need to include manufacturing defects?

Spray A: a second-generation Bosch common-rail injector
 (5 nominally identically devices donated to ECN)

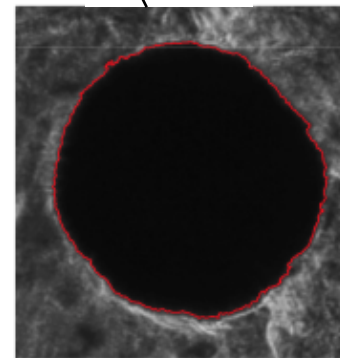


Phase contrast imaging of the orifice:
 the orifice is misaligned w.r.t. the
 injector and has irregular taper

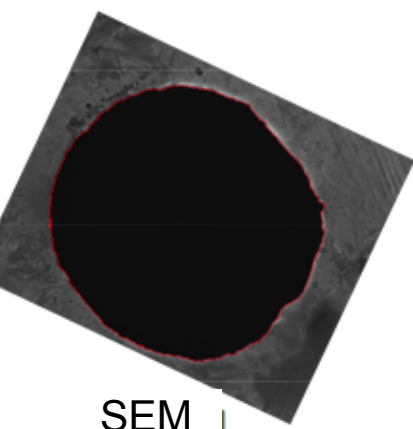


$\phi = 90 \mu\text{m}$

Orifice exit: holes are
 elliptical at the outlet,
 not round (2-7 μm)



Optical microscopy



SEM